ISME

Nonlinear Non-minimum Phase Flight Vehicle Control Using Dynamic Sliding Manifold

B. Ebrahimi[*]
PhD Candidate

M. Bahrami[†]
Professor

J. Roshanian[‡]
Associated Professor

Design and synthesis of a nonlinear non-minimum phase supersonic flight vehicle longitudinal dynamics control for g commands output tracking are presented. The non-minimum nature of the resulting input/output pair necessitates using a modified switching manifold in sliding mode control theory. Dynamic sliding manifold is designed to compensate for unstable internal dynamics of the system associated with the coupling between the moment generating actuators and the aerodynamic forces on the flight vehicle. The employed method is simple to implement in practical applications and enables the sliding mode control design to exhibit the desired dynamic properties during the entire output-tracking process independent of matched perturbations and accommodates to unmatched perturbations. Results of simulations are presented to demonstrate the performance, robustness, and stability of the considered autopilot.

Keyword: Non-minimum Phase Systems; Internal Dynamics; Dynamic Sliding Mode; Disturbance

1 Introduction

Tail-controlled flight systems are commonly non-minimum phase systems that should be equipped with control systems whose task are to provide stability, disturbance attenuation, and reference signal tracking, while their aerodynamic coefficients vary over a wide dynamic range due to large Mach-altitude fluctuations and due to aerodynamic coefficient uncertainties resulting from inaccurate wind-tunnel measurements.

It is known that a nonlinear control system is non-minimum phase if its internal or zero dynamics are unstable [1]. The non-minimum phase characteristic of a plant restricts direct application of nonlinear control techniques such as feedback linearization and sliding mode control [2]. In general, exact tracking in causal nonlinear non-minimum phase systems seems to be impossible for arbitrary reference signals even in absence of plant uncertainties and external disturbances [3]. The problem of tracking a class of reference signals given by a known nonlinear exosystem is reduced to solving a first order partial differential algebraic equation [4]. Approximate solutions to this equation have been proposed in [5,6] and exact tracking of known trajectory via stable nonlinear non-causal inverse in [7].

It is common practice, when designing a control system for a non-minimum phase flight vehicle, to represent the flight envelope by a grid of Mach-altitude operating points and then to perform a linearization of the nonlinear state equations at trim points of the gridded flight

[*] Mechanical Engineering Department, Amirkabir University of Technology, Tehran, Iran
[†] Corresponding Author, Mechanical Engineering Department, Amirkabir University of Technology, Tehran, Iran
Email:mbahrami@aut.ac.ir
[‡] Aerospace Engineering Department, KNToosi University of Technology, Tehran, Iran

envelope. The plant becomes a differential inclusion under continuously varying flight conditions. There are many possible ways of dealing with the control of such linear non-minimum phase and time varying plants. The classical approach being to design a controller for a certain point and then to schedule the controller's gain to place eigenvalues deep in the left half plane and the near real-axis according to a measured or derived parameters that represent flight conditions, such as angle of attack or Mach number [8]. In another method, H_∞ methods are invoked to design a collection of controllers, where for each operating point in the flight envelope grid, a controller with a fixed structure result [9]. The ensuing set of controllers is then transformed to a single gain scheduled controller by obtaining a least-square fit of its parameters with respect to angle of attack, or Mach number, etc.For highly agile air vehicle, these techniques would result in an extensive number of controller design points to be able to cope with the drastically changing dynamic behavior throughout the flight envelop.

All of the aforementioned methods are linear design techniques that require either exact knowledge of system parameters or, alternatively, assumption of some uncertainty model such as norm boundedness, thus allowing for robust controller design. On the other hand, sliding mode control may, in principle, be implemented for dynamic systems having only a qualitative description and a number of inequality restrictions. A radical departure from the conventional sliding mode control design philosophy is that a dynamic sliding manifold is utilized to accomplish design objectives beyond the capability of conventional sliding mode controllers for non-minimum phase systems [3]. As will be shown in sequel, this approach will provide a simple and high-performance controller on nonlinear system designed about a fixed operating point using straightforward design procedure. Sliding modes are the primary form of operational variable structure systems. A sliding mode is a motion on a discontinuity set of a dynamic system and is characterized by a suite of feedback control law and a decision rule known as switching function. Such modes are used to maintain the given constraints with utmost accuracy. The sliding mode controller is an attractive robust control algorithm due to its inherent insensitivity and robustness to plant uncertainties and external disturbances.

The nonlinear pitch dynamics of a hypothetical tail-controlled flight vehicle is derived and rendered into a linear-time-varying system via classical linearization method in Sec. 2. In section 3 a proper set point is utilized to exploit Linear Time Invariant, LTI, system benefits. A practical application of dynamic sliding manifold is employed to circumvent restrictive performance of conventional sliding manifolds for the non-minimum phase pitch-axis dynamics of the air vehicle. The dynamic sliding mode control designed on the basis of the LTI system after successful results is employed for the nonlinear system to track commanded normal acceleration. The designed controller only requires actuator and tracking error variables. Robustness properties of the controller against nonlinearities and time variance are demonstrated in Sec. 4. The control robustness against aerodynamics coefficients variation is also evaluated.

2 Problem Formulation

The model employed in this analysis is based on the hypothetical tail-controlled air vehicle which has been used as a benchmark in a number of recent studies on nonlinear design techniques [8,11]. The control objective is to force the air vehicle to track a desired motion path generated by the guidance-navigation system as the reference acceleration commands for the center of the mass. The problem is first formulated and performance objectives are specified. The zero dynamics of the air frame is utilized to demonstrate the non-minimum characteristics of the system. The nonlinear pitch dynamics of a hypothetical tail-controlled

flight vehicle is then rendered into the Linear Time Varying, LTV, system via classical linearization method.

2.1 Dynamic Model of the Flight Airframe

The model assumes constant mass, no roll rate, zero roll angle, no side slip, and no yaw rate. Under these assumptions, the longitudinal nonlinear equation of motion is reduced to two forces and one moment. Using body axis coordinates, Fig. 1, these equations are

$$F_x = QSC_D \tag{1}$$

$$F_z = QSC_N \tag{2}$$

$$M_y = QSdC_M \tag{3}$$

The dynamic pressure is defined as

$$Q = \frac{1}{2}\rho V_v^2 = 0.7P_0M^2 \tag{4}$$

Note that velocity and air density are not assumed to be constant or slow-varying, but a standard atmospheric model is assumed in simulation based on previously reported data [12]. Aerodynamic polynomials resulting from wind-tunnel measurements are given as [8]

$$C_D = -0.3 \tag{5}$$

$$\begin{aligned} C_N[\alpha,\delta,M] &= \beta_{1N}\alpha^3 + \beta_{2N}\alpha|\alpha| + \beta_{3N}(2 - M/3)\alpha + d_n\delta \\ &= c_n(\alpha,M) + d_n\delta \end{aligned} \tag{6}$$

$$\begin{aligned} C_M[\alpha,\delta,M] &= \beta_{1M}\alpha^3 + \beta_{2M}\alpha|\alpha| + \beta_{3M}(-7 + 8M/3)\alpha + d_m\delta \\ &= c_m(\alpha,M) + d_m\delta \end{aligned} \tag{7}$$

The numerical values of the various constant parameters in the dynamic equations (5-7) are given in Table 1. Note that all coefficients are dimensionless and all angles are in radians. Consequently, the differential equations describing the body motion are

$$\dot{\alpha} = \frac{\cos\alpha}{mV_v}F_z + q \tag{8}$$

$$\dot{q} = \frac{M_y}{I_y} \tag{9}$$

$$a_z = \frac{F_z}{mg} \tag{10}$$

$$\dot{V}_v = \frac{F_x\cos\alpha}{m} - \left|\frac{F_z\sin\alpha}{m}\right| \tag{11}$$

$$\dot{h} = Mv_s\sin\gamma \tag{12}$$

$$\dot{X} = Mv_s\cos\gamma \tag{13}$$

The tail-fin actuator dynamics describing the tail deflection is

$$\dot{\delta} = \frac{1}{\tau_a}(\delta_c - \delta) \tag{14}$$

where actuator fin deflection is limited to - 40° ≤ δ ≤ 40°. Table 2 gives the flight vehicle constants.

As shown in the equations of motion, the time-varying aerodynamic parameters contribute heavily to the variation of dynamic forces and moments exerted on the vehicle airframe. It is assumed here as is often customary in air vehicle autopilot design that the vehicle velocity (or Mach number) is constant and the nonlinear state equation associated with V_v is dropped from the design model [11]. In this case, the vehicle velocity becomes an independent (external) parameter upon which the state dynamics depend.

By rewriting equations (8) to (10), it is easy to show that

$$\begin{aligned} \dot{\alpha}(t) &= K_\alpha M C_N[\alpha(t), \delta(t)]cos[\alpha(t)] + q(t) \\ \dot{q}(t) &= K_q M^2 C_M[\alpha(t), \delta(t)] \\ \dot{\delta}(t) &= \frac{1}{\tau_a}[\delta_c(t)-\delta(t)] \\ a_z(t) &= K_z M^2 C_N[\alpha(t), \delta(t)] \end{aligned} \tag{15}$$

where $K_\alpha = \frac{0.7P_0S}{mv_s}$, $K_q = \frac{0.7P_0Sd}{I_y}$, $K_z = \frac{0.7P_0S}{m}$. The numerical values of constant parameters are listed in Table 3 at an altitude of 6100 m (20,000 ft).

2.2 Performance Objectives

The control objective is to force the air vehicle to track a desired motion path. To this end, the guidance-navigation system generates the reference acceleration commands for the center of the mass, denoted as a_z^{com}. This reference acceleration is compared with the actual normal acceleration measured in order to reveal a tracking error. The control problem consists of generating a tail deflection δ_c, which produces the angle of attack that corresponds to the required maneuver. Considering the air vehicle flying at an altitude of 6100 m (≈ 20,000 ft); the closed-loop system should maintain stability over the operating range specified by [$\alpha(t)$, $M(t)$] such that -30° ≤ $\alpha(t)$ ≤ 30° and 2 ≤ $M(t)$ ≤ 4.

2.3 Input/Output linearization

The longitudinal model of the flight vehicle described by Eq. (15) is a special case of a general nonlinear system of the form

$$\begin{aligned} \dot{\boldsymbol{x}}(t) &= f(\boldsymbol{x}) + g(\boldsymbol{x})u \\ y &= h(\boldsymbol{x}) \end{aligned} \tag{16}$$

where *f, g,* and *h* are sufficiently smooth functions of $\boldsymbol{x} \in \Re$.

Remark 1: Relative degree, *r* for nonlinear system (16), is defined as follows.

$$\begin{aligned} &\mathcal{L}_g \mathcal{L}_f^k h(\boldsymbol{x}) = 0, \qquad k < r\text{-}1 \\ &\mathcal{L}_g \mathcal{L}_f^{r-1} h(\boldsymbol{x}) \neq 0 \end{aligned} \tag{17}$$

Utilizing Eq. (17), the relative degree of the system (15) can be obtained as $r = 1 < n$ which states that the nonlinear system can only be partially linearized and stability of the system depends not only on the linearized system, but also on the stability of the internal dynamics (zero dynamics). System of Eqs. (15) can be transformed into the normal form using a nonlinear mapping $z = \mathbf{\Phi}(\boldsymbol{x})$ such that [1]:

$$\begin{aligned} \boldsymbol{z} &= \left[\zeta(t) \quad \eta_1(t) \quad \eta_2(t)\right]^{\mathrm{T}} \\ \mathbf{\Phi}(\boldsymbol{x}) &= \left[a_z(t) \quad \alpha(t) \quad q(t)\right]^{\mathrm{T}} \end{aligned} \tag{18}$$

Corresponding input/output and internal dynamics can be obtained as

$$\begin{aligned} \dot{\zeta} &= \mathcal{L}_f h(\boldsymbol{x}) + \mathcal{L}_g\, h(\boldsymbol{x}).u(t) \\ \dot{\eta}_i &= \mathcal{L}_f \Phi_j(\boldsymbol{x}),\ j = i+1 \text{ for } i = 1,\ 2 \end{aligned} \tag{19}$$

where $\Phi_j(\boldsymbol{x})$ are found such that $\mathcal{L}_g \Phi_j(\boldsymbol{x}) = 0$.

For the system of Eqs. (15), the input/output linearization and internal dynamics result in Eq. (20) and Eq. (21), respectively.

$$\begin{aligned} \dot{\zeta}(t) = K_1 \left[\frac{\partial c_n[\eta_1(t)]}{\partial \eta_1(t)} [K_2 \zeta(t)\eta_1(t) + \eta_2(t)] + K_3 c_n[\eta_1(t)] \right] \\ - K_3 \zeta(t) + K_4 \delta_c(t) \end{aligned} \tag{20}$$

$$\begin{aligned} \dot{\eta}_1(t) &= K_2 \zeta(t)\eta_1(t) + \eta_2(t) \\ \dot{\eta}_2(t) &= K_5 c_n[\eta_1(t)] + K_6 \zeta(t) \end{aligned} \tag{21}$$

where K_is are corresponding fixed and known coefficients. The zero dynamics are calculated from the internal dynamics by setting the output ζ to be zero. The zero dynamics of Eq. (21) may thus be calculated as

$$\ddot{\eta}_1(t) = K_5 c_n[\eta_1(t)] \tag{22}$$

Figure 2 illustrates a phase portrait of the zero dynamics, where a saddle point of the zero dynamics lies at (0,0). This corresponds to the equilibrium flight mode in which the air vehicle flies with a zero angle of attack when at constant velocity and constant altitude. For initial conditions starting on the saddle-like trajectories the angle of attack will follow an unbounded trajectory causing the air vehicle to turn somersault. Note that the two other equilibria $(\alpha, \dot{\alpha}) = (-0.187, 0)$ and $(\alpha, \dot{\alpha}) = (0.187, 0)$ correspond to unstable centers which for initial conditions starting in the vicinity of these equilibria, angle of attack follows unbounded periodic trajectory and the nose of the vehicle is forced to oscillate up and down. Consequently, it is deduced from the phase portrait that almost all initial conditions for α and its variation will result in solutions which are unstable. Hence, the conventional sliding mode based on the input-output linearization (20) and switching manifold as $s = e = \zeta^{\mathrm{com}} - \zeta$ will not be met for any bounded control.

2.4 Linear Description of the Flight Vehicle

In order to obtain the linear description of the flight airframe Eqs. (15) is linearized about equilibrium operating points $(\alpha, M, M_y = 0)$.

Simplify the problem by neglecting the actuator dynamics, assuming its bandwidth is sufficiently wide. Let

$$\boldsymbol{\xi}(t) = \begin{bmatrix} \xi_1(t) \\ \xi_2(t) \end{bmatrix} = \begin{bmatrix} \alpha(t) \\ q(t) \end{bmatrix} \tag{23}$$

where $\xi(t)$ is the state vector of the reduced-order nonlinear model. Then the state equation is given by

$$\dot{\boldsymbol{\xi}} = f(\boldsymbol{\xi}, \delta) = \begin{bmatrix} f_1(\xi_1, \xi_2, \delta) \\ f_2(\xi_1, \xi_2, \delta) \end{bmatrix} \qquad a_z = g(\boldsymbol{\xi}, \delta) = g(\xi_1, \xi_2, \delta) \tag{24}$$

where

$$f_1(\xi_1, \xi_2, \delta) = K_\alpha M(t) C_N[\xi_1, \delta, M] cos(\xi_1) + \xi_2$$

$$f_2(\xi_1, \xi_2, \delta) = K_q M^2(t) C_M[\xi_1, \delta, M]$$

$$g(\xi_1, \xi_2, \delta) = K_z M^2(t) C_N[\xi_1, \delta, M]$$

Now for a given commanded normal acceleration profile $a_z^{\text{com}}(t)$, let $\bar{\delta}(t)$ be the nominal tail-fin deflection and $\bar{\xi}(t)$ be the nominal state trajectory such that

$$\dot{\bar{\boldsymbol{\xi}}} = f[\bar{\boldsymbol{\xi}}(t), \bar{\delta}(t)] \qquad a_z(t) = g[\bar{\boldsymbol{\xi}}(t), \bar{\delta}(t)] \tag{25}$$

Define the tracking errors by

$$\boldsymbol{x}(t) = \boldsymbol{\xi}(t) - \bar{\boldsymbol{\xi}}(t) \qquad y(t) = a_z(t) - a_z^{\text{com}}(t) \tag{26}$$

and the tracking error control input by

$$v(t) = \delta(t) - \bar{\delta}(t) \tag{27}$$

Then the linearized tracking error dynamics are given by

$$\begin{aligned} \dot{\boldsymbol{x}} &= \mathbf{A}(t)\boldsymbol{x} + \mathbf{B}(t)v \\ y &= \mathbf{C}(t)\boldsymbol{x} + \mathbf{D}(t)v \end{aligned} \tag{28}$$

where

$$\mathbf{A}(t) = \left.\frac{\partial f}{\partial \boldsymbol{\xi}}\right|_{\bar{\xi},\, \bar{\delta}} = \begin{bmatrix} a_{11}(t) & 1 \\ a_{21}(t) & 0 \end{bmatrix} \tag{29}$$

with

$$\begin{aligned} a_{11}(t) = K_\alpha M(t)(&\{3\beta_{1N}\bar{\xi}_1^2(t) + 2\beta_{2N} \,|\, \bar{\xi}_1(t) \,| + \beta_{3N}[2 - M(t)/3]\} \\ &\times \cos[\bar{\xi}_1(t)] - \{\beta_{1N}\bar{\xi}_1^3(t) + \beta_{2N} \,|\, \bar{\xi}_1(t) \,|\, \bar{\xi}_1(t) \\ &+ \beta_{3N}[2 - M(t)/3]\bar{\xi}_1(t) + d_n\bar{\delta}\}\sin[\bar{\xi}_1(t)]) \end{aligned} \tag{30}$$

$$a_{21}(t) = K_q M^2(t)\{3\beta_{1M}\bar{\xi}_1^2(t) + 2\beta_{2M}\,|\,\bar{\xi}_1(t)\,| + \beta_{3N}[-7 + 8M(t)/3]\} \tag{31}$$

$$\mathbf{B}(t) = \left.\frac{\partial f}{\partial \delta}\right|_{\bar{\xi},\bar{\delta}} = \begin{bmatrix} b_1(t) \\ b_2(t) \end{bmatrix} = \begin{bmatrix} K_\alpha M(t) d_n \cos[\bar{\xi}_1(t)] \\ K_q d_m M^2(t) \end{bmatrix} \tag{32}$$

$$\mathbf{C}(t) = \left.\frac{\partial g}{\partial \boldsymbol{\xi}}\right|_{\bar{\xi},\bar{\delta}} = [c \quad 0] \tag{33}$$

with

$$c = K_z M^2(t)\{3\beta_{1\mathrm{N}}\bar{\xi}_1^2(t) + 2\beta_{2\mathrm{N}}\,|\,\bar{\xi}_1(t)\,| + \beta_{3\mathrm{N}}[2 - M(t)/3]\} \tag{34}$$

$$\mathbf{D}(t) = \left.\frac{\partial g}{\partial \delta}\right|_{\bar{\xi},\bar{\delta}} = d_n K_z M^2(t) \tag{35}$$

The obtained system is linear time varying and depends on the angle of attack and Mach number at each equilibrium point. It is common practice to choose multiple operating points to design a separate controller for each point and obtain the autopilot by integration of designed controllers. The method presented in this paper is a straight forward approach that requires only a proper design point and obliterates designing a multi-phase controller.

3 Autopilot Design Based on Dynamic Sliding Manifold

The resulted LTV model of the air vehicle can be evaluated at each design point to obtain a corresponding LTI model. In this analysis a proper design point will be shown sufficient to exhibit desired performance and resulting in a simple and robust autopilot dependant only on the actuator state variable and output tracking error. The dynamic sliding manifold is then designed based on the well-established LTI design methods and the corresponding autopilot is proposed to generate smooth actuator deflection.

The obtained LTV model (28) is dependant on the angle of attack and Mach number, generally, it is needed to grid the two-dimensional space (α,M) for synthesis purpose through a flight envelope. Note that the state-space entries are symmetric in terms of variable α; thus, only positive values of $\alpha(t)$ are considered. Grid points can be found by trial and error, or by using an expert's knowledge of operating conditions of the system. Also, fuzzy clustering can help designers find proper points [13]. Hence, an LTI model of the system accompanied by the actuator dynamics, Eq. (14), can be represented as follows:

$$\begin{aligned} \dot{\hat{\boldsymbol{x}}} &= \hat{\mathbf{A}}\hat{\boldsymbol{x}} + \hat{\mathbf{B}}\delta_c \\ \hat{y} &= \hat{\mathbf{C}}\hat{\boldsymbol{x}} + \hat{\mathbf{D}}\delta_c \end{aligned} \tag{36}$$

where

$$\begin{aligned} &\hat{\mathbf{A}} = \begin{bmatrix} \mathbf{A} & \mathbf{B} \\ \mathbf{0} & -1/\tau_a \end{bmatrix}, \qquad \hat{\mathbf{B}} = \begin{bmatrix} \mathbf{0} \\ 1/\tau_a \end{bmatrix} \\ &\hat{\mathbf{C}} = [\mathbf{C} \quad \mathbf{D}], \qquad \hat{\mathbf{D}} = \mathbf{0} \end{aligned} \tag{37}$$

$\hat{\boldsymbol{x}} = [\boldsymbol{x} \;\; \delta]^{\mathrm{T}}$ and δ_c is the control function. **A**, **B**, **C**, and **D** are constant matrices evaluated for a specified design point. (**A**, **B**) is a controllable pair; and a_z^{com} is a reference output profile.

Following the approach by Shtessel et al. [10], the aim is to specify a sliding mode control

$$\delta_c = \begin{cases} \delta_c^+, & \Im(\boldsymbol{x}, a_z^{\text{com}}, t) > 0 \\ \delta_c^-, & \Im(\boldsymbol{x}, a_z^{\text{com}}, t) < 0 \end{cases} \tag{38}$$

where $\Im(\boldsymbol{x}, a_z^{\text{com}}, t)$ is dynamic sliding manifold acting on actuator states and on output tracking error of the system; δ_c^+, δ_c^- are continuous functions of x and t, to accomplish the motion of tracking error $e(t)= a_z^{\text{com}}(t)-a_z(t)$ on sliding manifold $\Im = 0$ with given eigenstructure and providing existence of sliding manifold. Consider the dynamic sliding manifold $\Im$ represented by

$$\ddot{\Im} + \kappa.\dot{\Im} = \dddot{\delta} + a.\ddot{\delta} + b.\dddot{e} + c.\ddot{e} + d.\dot{e} \tag{39}$$

where a, b, c, d, κ are constant parameters designed to compensate for unstable internal dynamics of the system associated with the coupling between the moment generating actuators and the aerodynamic forces on the flight vehicle.

Existence condition of sliding mode, $\Im\dot{\Im} < -\rho\,|\,\Im\,|$, must be met in the vicinity of the sliding manifold [14]. This is obtained for the system (36) and (38) as follows in Eq. (40) with $\kappa = a$ for the sake of simplicity.

$$\begin{aligned} &\ddot{\delta}_c + (a - 1/\tau)\dot{\delta}_c \\ &\quad = (a - 1/\tau)\ddot{\delta} - \tau[b.\dddot{e} + c.\ddot{e} + d.\dot{e} + a.\mu.\text{sgn}(\Im)] \end{aligned} \tag{40}$$

In order to design constant parameters, it is assumed that the switching surface $\Im$ is representable as a transfer function

$$\Im = \delta + \frac{Q(s)}{P(s)} e \tag{41}$$

where s=*d*/*dt*, Q(s) and P(s) are polynomials of s and design parameters of dynamic sliding manifold. To obtain the polynomials for sliding manifold structure, the state tracking error output is constructed as

$$E(s) = \frac{P(s)}{P(s) - [\mathbf{D} + \mathbf{C}(\mathbf{sI} - \mathbf{A})^{-1}\mathbf{B}]Q(s)} a_z^{\text{com}}(s) \tag{42}$$

Remark 2: The polynomials *Q*(s), *P*(s) must be identified to provide the following desired features to the non-minimum phase output tracking.

1) The eigenvalues of the closed loop control system must be placed at desired locations:

$$P(s) - [\mathbf{D} + \mathbf{C}(\mathbf{sI} - \mathbf{A})^{-1}\mathbf{B}]Q(s) = 0 \tag{43}$$

2) The tracking error must not exhibit any steady state error.

$$e_{ss} = \lim_{s \to 0} s \frac{P(s)}{P(s) - [\mathbf{D} + \mathbf{C}(\mathbf{sI} - \mathbf{A})^{-1}\mathbf{B}]Q(s)} a_z^{\text{com}}(s) = 0 \tag{44}$$

This condition can be easily met if type of $a_z^{\text{com}}(t)$ is known as $t \to \infty$. Provided that the polynomials *Q*(s), *P*(s) are designed to meet condition (43), and the discontinuous control

(38) meets the existence condition, the sliding mode exists in the dynamic sliding manifold (39) achieves the desired output tracking of the non-minimum phase system.

In aeronautical applications avoidance of any possible excitation of structural modes by the high frequency operation of the control is of extreme importance. Although for the case studied in this analysis, smooth deflection of the actuator is provided by the low pass characteristics of the transfer function of the actuator, but to eliminate the chattering phenomena by the control, saturation control operating within a thin boundary layer ε is utilized as

$$\delta_c = \Omega \text{sat}\left(\frac{\Im}{\varepsilon}\right) \tag{45}$$

where $\Omega > |u_{eq}| + \iota,\ \forall \iota > 0$ and u_{eq} obtained using Eq. (40).

In practice, fast tracking performance for abrupt guidance command trajectories is always constrained by the physical limit of the actuator rate. A common practice in coping with this dilemma is to use a tracking command filter. The filter should greatly reduce the acceleration and rate of the abrupt command trajectory [**11**]. In this analysis a second order filter is utilized in simulation process for a sequence of step commands in acceleration as

$$\frac{a_{z_f}^{com}}{a_z^{com}} = \frac{\omega_n^2}{s^2 + 2\varsigma\omega_n s + \omega_n^2} \tag{46}$$

4 Simulation Results

Consider Eq. (36) linearized at the design-point (α=7°,M=4). This point can be found by trial and error or by using fuzzy clustering approach [13].

$$\mathbf{A} = \begin{bmatrix} -1.07 & 1 \\ -61.4 & 0 \end{bmatrix}, \quad \mathbf{B} = \begin{bmatrix} -0.16 \\ -232.65 \end{bmatrix}$$
$$\mathbf{C} = [-1380 \quad 0], \quad \mathbf{D} = -203.7 \tag{47}$$

The non-minimum phase transfer function of the system is obtained as

$$\frac{a_z}{\delta} = \frac{-204(s - 38.91)(s + 38.9)}{s^2 + 1.07s + 61.4} \tag{48}$$

The polynomials of dynamic sliding manifold are designed to provide the eigenvalue placement as required for characteristic Eq. (43) as well as to nullify steady state error. Eigenstructure assignment based on the Deadbeat response criteria, or Integral of Time multiplied by the Absolute magnitude of the Error, ITAE, criteria may be utilized. Using the deadbeat index, polynomials Q(s) and P(s) are designed as follows:

$$Q(s) = -0.0018s^2 - 0.022s - 0.17$$
$$P(s) = s^2 + 25.8s \tag{49}$$

The second order filter (46) is utilized with $\omega_n = 10$ and $\varsigma = 0.7$ for a sequence of abrupt step commands.

Output tracking performance and control behavior for linear system (47) has been demonstrated in Fig. 3 for a sequence of step commands in normal acceleration. After successful design of dynamic sliding mode control for linearized system, the next step is to evaluate the controller's performance on the nonlinear system. It is expected that the performance of the nonlinear closed-loop system will agree with that of the linearized system due to the robustness properties of the sliding mode control against nonlinearities and time variances. Response $a_z(t)$ of the nonlinear closed system, with the controller designed to a series of step and sinusoidal commands a_z^{com}, and the corresponding variations in the angle of the attack, Mach number, pitch rate, altitude, and actuator tail deflection are shown in Fig. 4 and 5, respectively.

Figure 6, shows step responses for the four possible combinations of ± 30% variation in the two aerodynamic coefficients $c_n(\alpha,M)$ and $c_m(\alpha,M)$, indicating excellent robustness of the closed loop system against perturbations and parameter variations.

Although the autopilot has been designed for altitude of 6,100m (≈20,000 ft), but in reality the air vehicle has to operate over a wide range of altitudes. To demonstrate the autopilot ability to face such situations the vehicle operation is checked for altitudes of approximately, 7,500m and 3,500m as well and the resulted performance demonstrated in Fig. 7.

5 Conclusion

In the non-minimum phase nonlinear systems, namely systems with unstable zero dynamics, perfect tracking via direct inversion of the input/output dynamics cannot be achieved. Accordingly, existence condition of conventional sliding modes cannot be met for any bounded control completely and the system experiences instability due to unstable internal dynamics. To circumvent this problem for the flight vehicle considered, the dynamic sliding manifold is utilized and its excellent performance demonstrated by simulation results for longitudinal pitch dynamics. The simple and straightforward design procedure, together with the encouraging robustness against nonlinearities and parameter variations resulted from simulation results; invite further application of this approach. It has to be stressed that the employed controller requires only actuator state variable and normal acceleration output tracking error, whose measurements are accomplished using simple instrumentations.

References

[1] Isidori, A. "Nonlinear Control Systems, Springer," (1995).

[2] Utkin, V. I., Guldner, J., and Shi J., "Sliding Modes in Electromechanical Systems," Taylor and Francis, London, (1998).

[3] Shkolnikov, I. A., and Shtessel, Y., "Tracking in a Class of Non-minimum Phase Systems with Nonlinear Internal Dynamics via Sliding Mode Control using Method of System Center," Automatica, Vol. 38, pp. 837-842, (2002).

[4] Byrnes, C. I., and Isidori, A., "Output Regulation for Nonlinear Systems: An Overview," International Journal of Robust and Nonlinear Control, Vol. 10, pp. 323-337, (2000).

[5] Shkolnikov, I. A., and Shtessel, Y., "Tracking Controller Design for a Class of Non-minimum Phase Systems via the Method of System Center," IEEE Transaction on Automatic Control, Vol. 46, No. 10, pp. 1639-1643, (2001).

[6] Gopalswmy, S., and Hedrick, J. K., "Tracking Nonlinear Non-minimum Phase System Using Sliding Control," International Journal of Control, Vol. 57, No. 5, pp. 1141-1158, (1993).

[7] Devasia, S., Chen, D., and Paden, B., "Nonlinear Inversion-based Output Tracking," IEEE Transaction on Automatic Control, Vol. 41, pp. 930-942, (1996).

[8] Mehrabian, A. R., and Roshanian, J., "Skid-to-turn Missile Autopilot Design using Scheduled Eigenstructure Assignment Technique," Journal of Aerospace Engineering, Imech Part G, Vol. 220, pp. 225-239, (2006).

[9] Nichols, R. A., Richert, R. T., and Rugh, W. J., "Gain Scheduling for H_∞ Controllers: A Flight Control Example," IEEE Transaction on Control Systems Technology, Vol. 1, No. 2, pp.69-79, (1993).

[10] Shtessel, Y. B., "Nonlinear Output Tracking in Conventional and Dynamic Sliding Manifolds," IEEE Transaction on Automatic Control, Vol. 42, No. 9, pp. 1282-1286, (1997).

[11] Zhu, J. J., and Mickle, M. C., "Missile Autopilot Design using a New Linear Time-varying Control Technique," Journal of Guidance, Control, and Dynamics, Vol. 20, No. 1, pp. 150-157, (1997).

[12] US Standard Atmosphere, (US government printing office, Washington, D. C), (1976).

[13] Oesterom, M., and Babuska, R., "Design of a Gain Scheduling Mechanism for Flight Control Laws by Fuzzy Clustering," Control Engineering Practice, Vol. 14, No. 7, pp. 769-781, (2006).

[14] Decarlo, R., Zak, S. H., and Matthews, G. P., "Variable Structure Control of Nonlinear Multivariable Systems: A Tutorial," IEEE Proceedings, Vol. 76, No. 3, pp. 212-232, (1988)

Nomenclature

a_z^{com}	commanded normal acceleration, g
a_z	actual normal acceleration, g
d	reference diameter, m
g	gravity, m/s^2
h	altitude, m
m	vehicle mass, kg
q	pitch rate, rad/s
v_s	speed of sound, m/s
C_D	axial force dimensionless aerodynamic polynomial
C_N	normal force dimensionless aerodynamic polynomial
C_M	pitching moment dimensionless aerodynamic polynomial
F_x	axial force, N

F_z	normal force, N
I_y	moment of inertia, kg m^2
K_α, K_q, K_z	vehicle constant parameters
M	Mach number
M_y	pitching moment, N.m
P_o	static pressure, N/m^2
Q	dynamic pressure, kg/m s^2
S	reference surface area, m^2
V_v	speed of vehicle, m/s

Greek Symobls

α	angle of attack, rad
β_{1N}, β_{2N}, β_{3N}	angle of attack component of normal force dimensionless aerodynamic polynomial coefficients
β_{1M}, β_{2M}, β_{3M}	angle of attack component of pitching moment dimensionless aerodynamic polynomial coefficients
θ	pitch angle, rad
γ	flight path angle, rad
δ	actual tail fin deflection, rad
δ_c	commanded tail fin deflection, rad
ρ	air density, kg/m^3
τ_a	tail actuator time constant, sec
ξ_1, ξ_2	state variables for α and q
η_1, η_2	internal dynamics variables
ζ	output variable in normal form coordinates
Ω	control gain
σ	dynamic operator
$\Im$	dynamic sliding manifold

Tables

Table 1. Aerodynamic polynomial coefficients

β_{1N} = 19.3734	β_{1M} = 40.4396
β_{2N} = 31.0225	β_{2M} = -64.0147
β_{3N} = -9.717	β_{2M} = 2.9221
d_n = -1.9481	d_m = -11.8029

Table 2. Flight vehicle constants

Symbol	Value
I_y	247.43662 kg m^2
d	0.2286 m
S	0.0409 m^2
m	204.108 kg
τ_a	1/150 s
g	9.81 m/s^2

Table 3. Constant parameters at an altitude of 6100 m

Symbol	Approximate value
K_α	0.020691 s^{-1}
K_q	1.2326 s^{-2}
K_z	6.5363 m s^{-2}

Figures

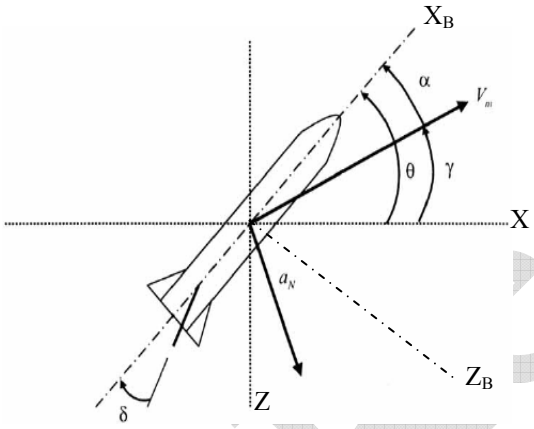

Figure 1 Airframe and dynamic variables

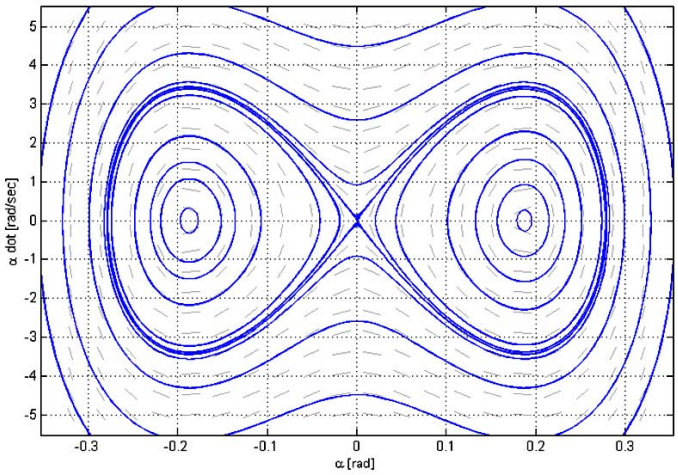

Figure 2 Phase portrait of zero dynamics

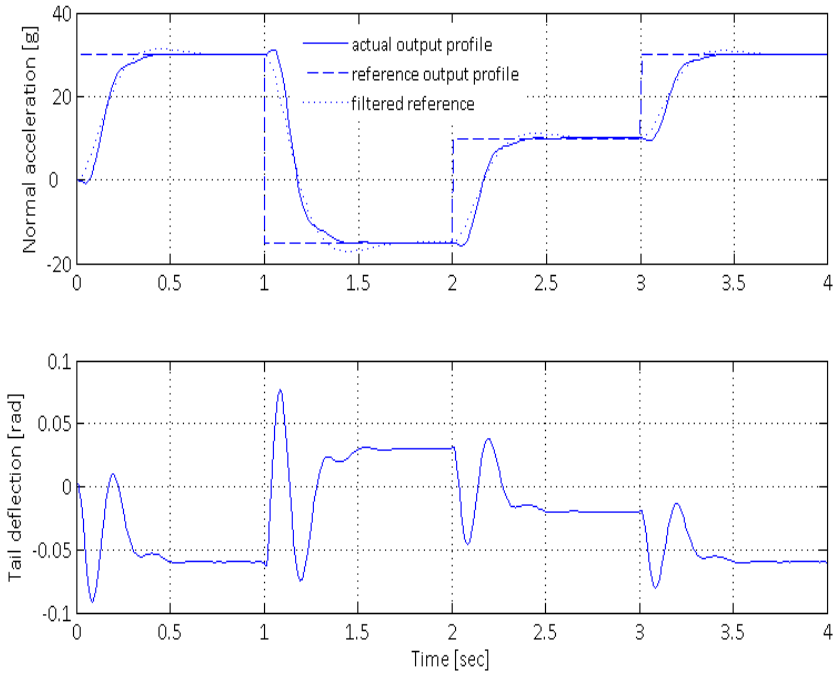

Figure 3 Linear system response to a sequence of step commands in acceleration

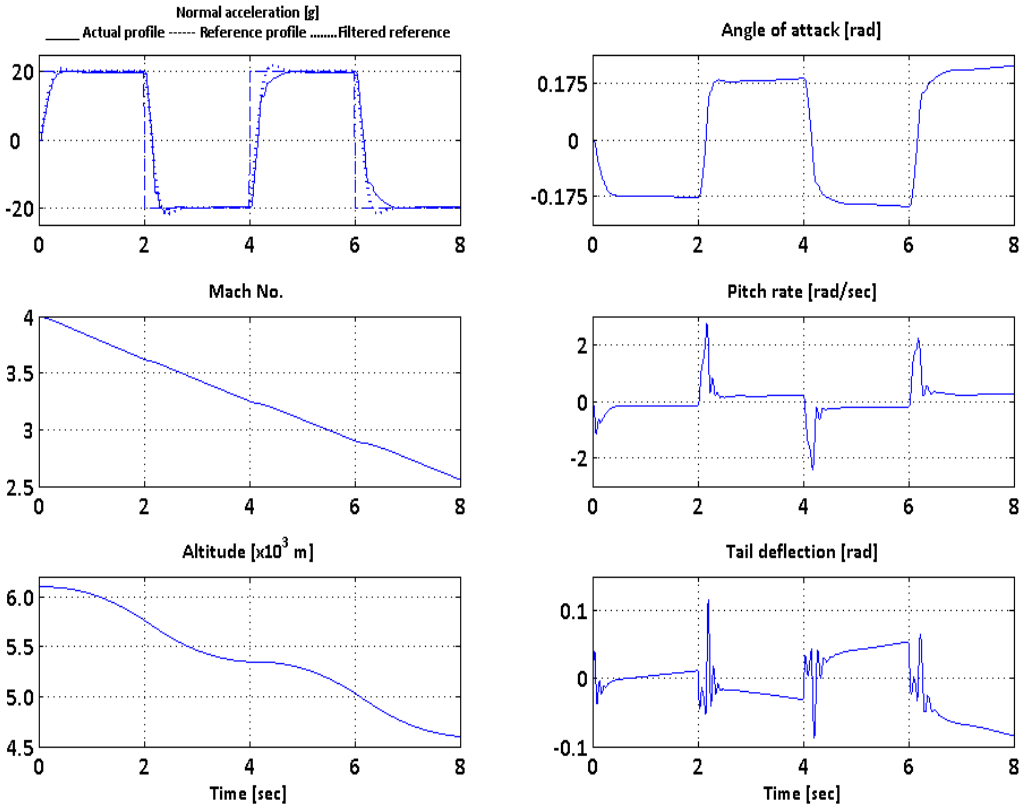

Figure 4 Nonlinear system response to a sequence of step commands in acceleration

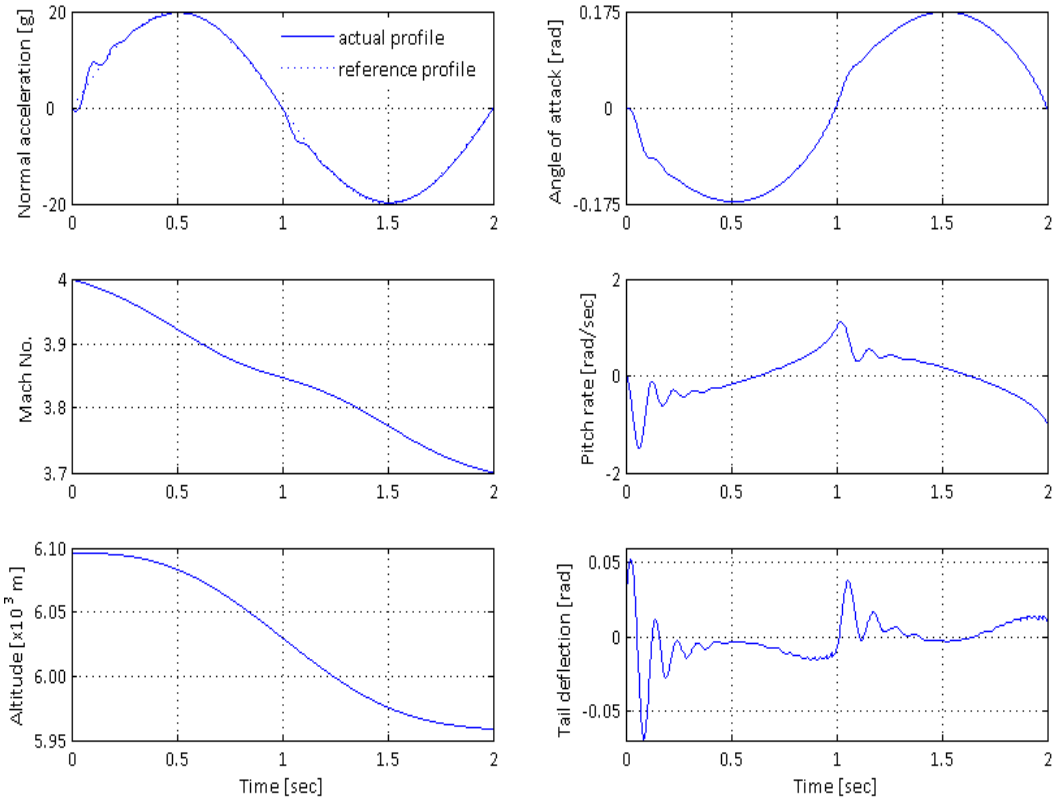

Figure 5 nonlinear system responses to a sinusoidal command in acceleration

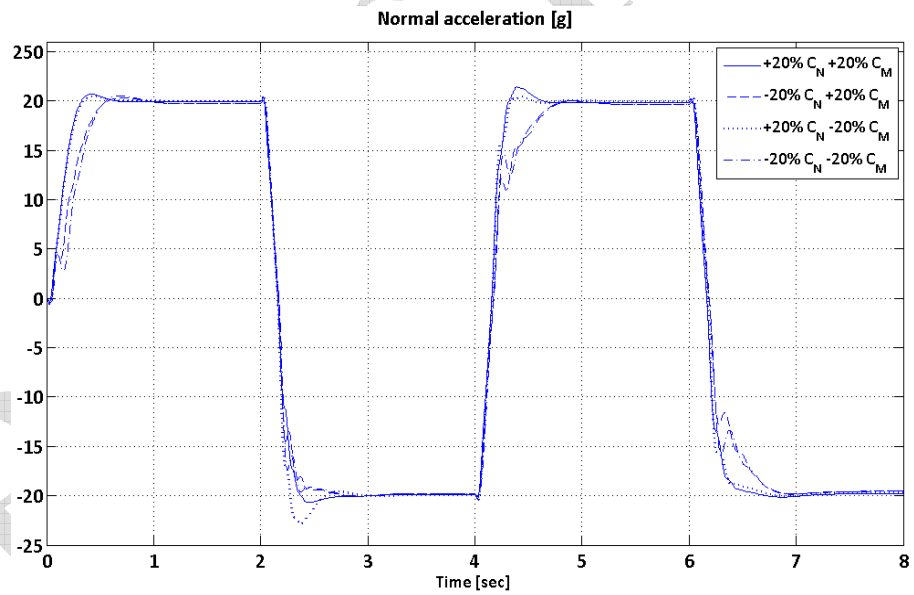

Figure 6 Nonlinear system response to a sequence of step commands in acceleration with perturbations in aerodynamic coefficients

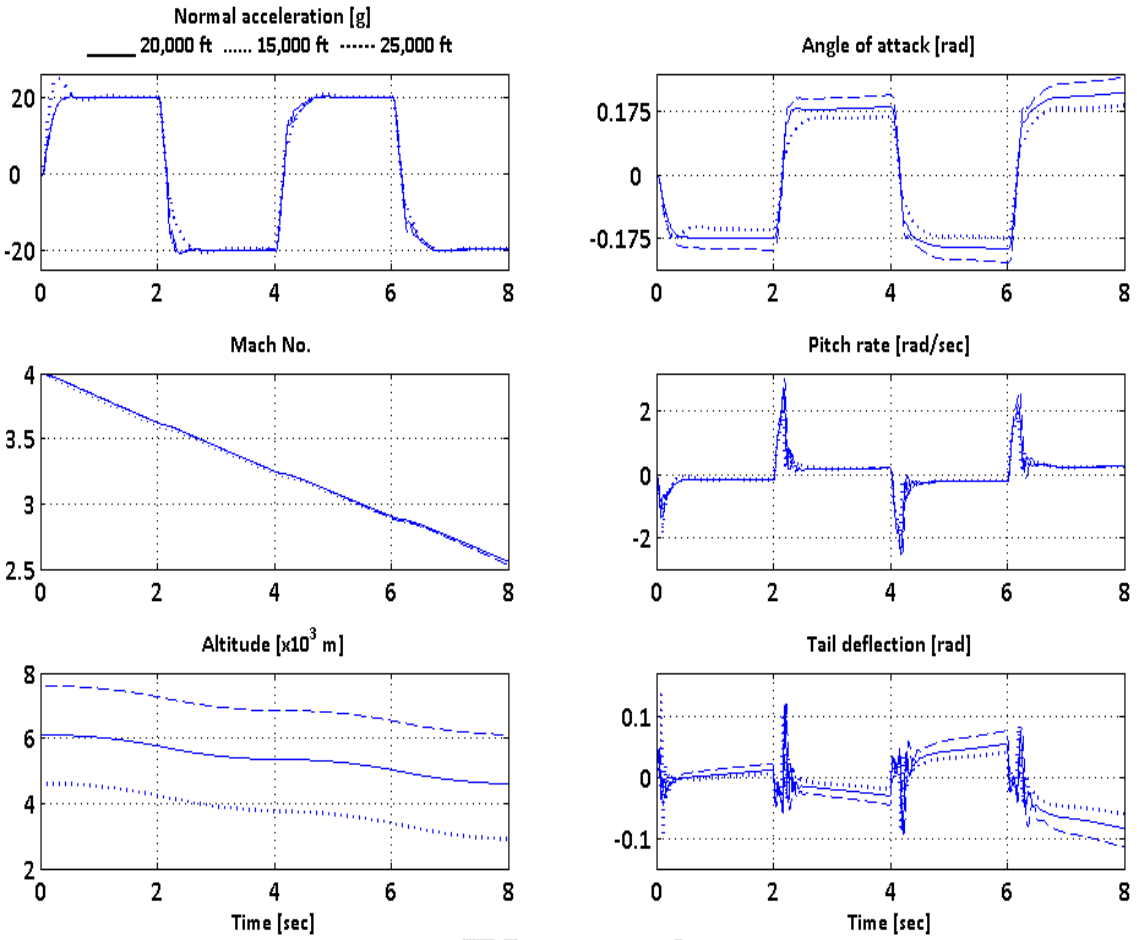

Figure 7 Nonlinear system response to a sequence of step commands in acceleration with different initial altitudes

چكيده

در اين مقاله طراحي كنترل ديناميک طولي يک موشک غيرخطي ناكمينه فاز مافوق صوت براي رديابي شتاب خروجي ارائه خواهد شد. رفتار ناكمينه فاز ورودي-خروجي ضرورت استفاده از منيفولد سوئيچي متفاوتي را در تئوري كنترل مد لغزشي مطرح مي سازد. بدين منظور از منيفولد لغزشي ديناميكي بمنظور جبران ديناميک داخلي ناپايدار موشک كه منشأ آن كوپلينگ بين عملگرهاي ايجاد كننده ممان و نيروهاي آيروديناميكي مي باشد، استفاده خواهد شد. بكار گيري روش ارائه شده در عمل ساده بوده و كنترل مد لغزشي را قادر مي سازد تا رفتار ديناميكي مطلوب را در طول زمان عملكرد موشک مستقل از اغتشاشات سازگار و ناسازگار فراهم آورد. در ادامه نتايج شبيه سازي براي چگونگي عملكرد، مقاوم بودن سيستم و پايداري اتوپايلوت مورد نظر ارائه خواهد شد.